Multifunctional silicon-based light emitting device in standard complementary metal–oxide–semiconductor technology*

Wang Wei(王 伟)†, Huang Bei-Ju(黄北举), Dong Zan(董 赞), and Chen Hong-Da(陈弘达)

State Key Laboratory on Integrated Optoelectronics, Institute of Semiconductors, Chinese Academy of Sciences, Beijing 100083, *China*

(Received 15 March 2010; revised manuscript received 13 August 2010)

A three-terminal silicon-based light emitting device is proposed and fabricated in standard 0.35 μm complementary metal–oxide–semiconductor technology. This device is capable of versatile working modes: it can emit visible to near infra-red (NIR) light (the spectrum ranges from 500 nm to 1000 nm) in reverse bias avalanche breakdown mode with working voltage between 8.35 V–12 V and emit NIR light (the spectrum ranges from 900 nm to 1300 nm) in the forward injection mode with working voltage below 2 V. An apparent modulation effect on the light intensity from the polysilicon gate is observed in the forward injection mode. Furthermore, when the gate oxide is broken down, NIR light is emitted from the polysilicon/oxide/silicon structure. Optoelectronic characteristics of the device working in different modes are measured and compared. The mechanisms behind these different emissions are explored.

Keywords: optoelectronic integrated circuit, complementary metal–oxide–semiconductor technology, silicon-based light emitting device, electroluminescence

PACS: 85.60.–q, 85.60.Jb **DOI:** 10.1088/1674-1056/20/1/018503

1. Introduction

In recent years, much attention has been paid to the silicon-based light emitting device (Si-LED) in the mainstream microelectronic process, owing to its promising application as a light source in all-silicon optoelectronic integrated circuits (OEIC). Continuous effort has been applied to making silicon emit light.[1−5] However, the fabrication processes of most these Si-LEDs are relatively complicated, which makes the advantage of monolithic integration less obvious. Since 1997, Snyman *et al.* have proposed and demonstrated many varied reverse bias Si-LEDs[6−8] in standard complementary metal–oxide–semiconductor (CMOS) technology. However the working voltages of these devices are too high to be compatible with the typical power supply of integrated circuits (IC). To further lower the working voltage and improve the conversion efficiency, Lee and Liu adopted LEDs under the forward injection mode.[9] Although not very efficient in comparison with III–V compound material, these Si-LEDs have the advantages of simplified fabrication process and reduced cost due to their full compatibility with standard CMOS technology.

Here we investigate Si-LEDs in standard CMOS technology, and propose a kind of three-terminal (p, n and polysilicon gate) LED which is capable of versatile working modes and emission characteristics. The optoelectronic characteristics of the device working in different modes are measured and compared. The mechanisms behind these varied emissions are discussed in depth.

2. Device structure

The design and fabrication process of this device are completely compatible with standard CMOS technology. The device structure is shown in Fig. 1. It consists of a series of interdigital shallow n^+ and p^+ type U-shaped semi-rings (n^+ and p^+ regions are realised at the same process with the source/drain region of a metal oxide semiconductor field effect transistor (MOSFET)). The n^+ and p^+ active regions are all embedded in an N-well in the bulk P-substrate. Here the N-well can isolate the substrate from the effect of the pn junction current. The U-shaped polysilicon (poly-Si, used for the gate of the MOSFET) strips are

*Project supported by the National Natural Science Foundation of China (Grant Nos. 60536030, 61036002, 60776024, 60877035 and 61036009) and National High Technology Research and Development Program of China (Grant Nos. 2007AA04Z329 and 2007AA04Z254).

†Corresponding author. E-mail: wangweiww33@semi.ac.cn

© 2011 Chinese Physical Society and IOP Publishing Ltd

deposited on the gate oxide between p^+/p^+ regions. From the cross-sectional view in Fig. 1(b) we can see that the structure constituted by the p^+ region and poly-Si is similar to several pMOSFETs in parallel. All the n^+ active regions in the N-well are connected to the 'cathode', and all the p^+ active regions in the N-well are connected to the 'anode' to constitute a multi p^+/N-well junction diode. The poly-Si gate as the third terminal can be either floating or connected to a variable voltage. It is expected to have a modulation effect on the output light intensity. The distance between each p^+ region and its neighbouring p^+ regions is about 0.6 μm and its neighbouring n^+ regions is 1 μm. The total area of the device is about 50 μm×55 μm.

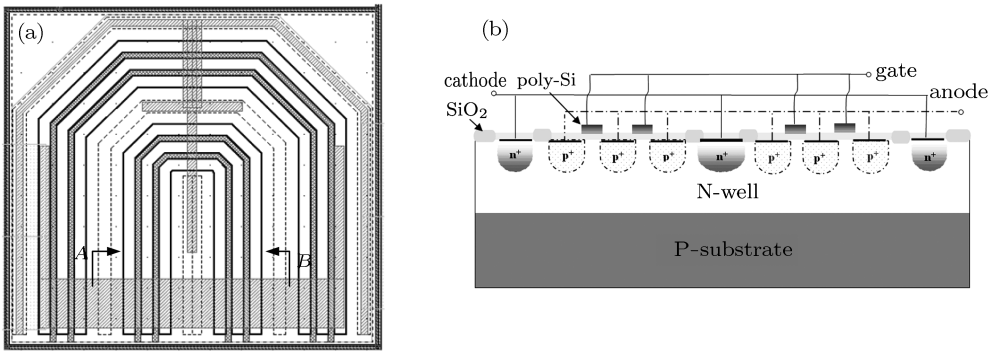


Fig. 1. The Si-LED structure. (a) Top view of the device, (b) cross-sectional view of the device (A–B section).

3. Device test

The device is fabricated in 0.35 μm 2P4M CMOS technology supplied by Chartered Semiconductor. The fabricated device can emit light in both reverse bias mode and forward bias mode. We investigate its optical and electrical characteristics in detail.

3.1. Light emission in reverse bias mode

The current versus reverse bias (I–V) and parasitic capacitance versus reverse bias (C–V) properties of the device are measured as shown in Fig. 2.

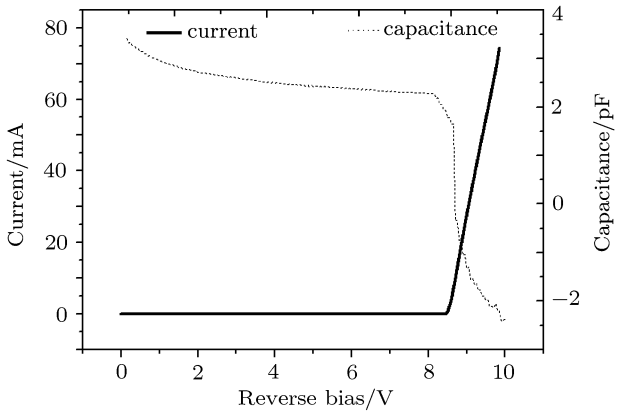


Fig. 2. The I–V and C–V characteristics in reverse bias mode.

The I–V characteristic shows the apparent avalanche breakdown property with breakdown point at about 8.35 V. If the applied bias is in excess of 12 V, the device can be damaged permanently due to heat breakdown. The total capacitance of the device is less than 3 pF. Taking the dynamic series resistance into account, we find that the device has an inherent frequency capability of gigahertz in theory.

Within the operating voltage range (8.35 V–12 V), the device can emit yellowish light on the junction edge clearly visible to the naked eye in slightly dimmed ambience, and a microphotograph of its lighting (at 10 V, 100 mA) is shown in Fig. 3. A typical electroluminescence (EL) spectrum of this device at current of 100 mA is shown by the solid line in Fig. 4., from which we can see that the range of emitting light wavelength (500 nm–1000 nm) is extended beyond the visible light domain with two main peaks at 801 nm (corresponding to photon energy of 1.548 eV) and 842 nm (1.473 eV). No significant shift of peak is observed as the current increases. There are many periodical minor peaks observed in the emission spectrum, which are attributed to Fabry–Perot (F–P) interference caused by the surface passivation layer. The spectral distribution and its peaks are a little different from the spectral peaks reported by Snyman *et al.*

in Ref. [10] which presents a peak at about 650 nm (1.91 eV). The total output optical power of our device is about 12.1 nW at 10 V, 100 mA and it increases almost linearly with the current through the device within working range and becomes saturated near the heat breakdown. The electric-optical conversion efficiency $\eta_{\rm p}$ and external quantum conversion efficiency (EQE) $\eta_{\rm ex}$ are about 1.2×10^{-8} and 7.8×10^{-8}, respectively. According to our estimation the real value is beyond that, since losses caused by the surface reflection measuring instrument are not taken into account.



Fig. 3. Microphotograph of LED in reverse bias mode.

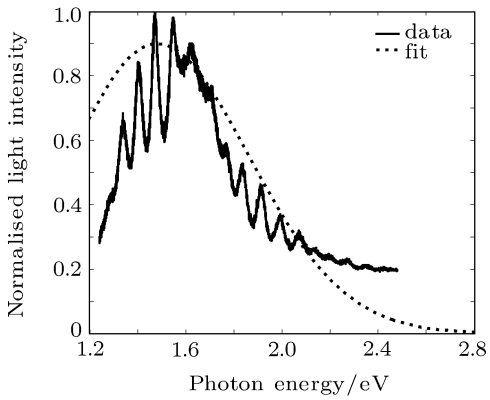


Fig. 4. EL spectra of the device in reverse bias mode. Experimental spectrum: solid line; theoretical fit: dashed line.

The mechanism behind the light emission under the avalanche breakdown condition is complicated. Although research on it can be traced back to 1955,[11] the photon generation mechanism of this phenomenon is still not conclusive.[12–14] In recent years, Akil *et al.* have proposed a multi-mechanism model[15] to explain the emission properties under avalanche breakdown. This model breaks the emission photon energy into three intervals: (i) indirect interband transitions (below 2 eV); (ii) intraband transitions, mainly Bremsstrahlung process (between 2 eV and 2.3 eV); (iii) direct interband transitions (beyond 2.3 eV). However there are some problems with this model, since according to Chynoweth and McKay,[16] although intraband transitions have a maximum photon energy of ≈ 2.3 eV theoretically, there is no measurable lower limit on energies of photons intraband ('c–c') transitions. But in Ref. [15] there is no definite explanation as to how to draw the line between different energy segments, and the classification of energy intervals cannot apply to various peaks in the pn junction under avalanche breakdown. Furthermore, models corresponding to a specific energy segment are monotonic at the entire emission range, which seems to be disputable. The spectrum derived from our device has different peaks from those previously reported, and its spectrum decreases greatly up to 2.3 eV which is principally the upper limit for intraband transitions; thus we presume that our emission is mainly ascribed to an indirect intraband transition combined with the absorption effect of the emitted light within the sample. The indirect intraband physical model proposed in Ref. [17] is used to fit the experimental result. Taking into account the silicon self-absorption effect, we obtain the EL intensity as

$$\mathrm{EL}(\hbar\omega)\propto \exp[-\alpha(\hbar\omega)\cdot d]\int_0^{\hbar\omega-\varepsilon_{\rm p}} dR(\hbar\omega), \qquad (1)$$

where $\hbar\omega$ is the emitted photon energy, d is the depth junction under the semiconductor surface, $\alpha(\hbar\omega)$ is the absorption coefficient given for an indirect band gap, $dR(\hbar\omega)$ is the photon emission rate and $\varepsilon_{\rm p}$ is the phonon energy. For silicon, phonon energies are neglected in comparison with the emitted photons energy; then the photon emission rate is given by

$$dR(\hbar\omega)\propto\hbar\omega\rho(\varepsilon_{\rm i})f(\varepsilon_{\rm i})[1-f(\varepsilon_{\rm i})]{\rm d}\varepsilon_{\rm i}, \qquad (2)$$

where $\rho(\varepsilon_{\rm i})$ is the state density which is equal to the product of the initial and final densities of electron states in the conductance band (CB), $f(\varepsilon_{\rm i})$ is the hot carrier distribution obtained by taking into account the electron interaction with acoustic and optical phonons. For a more detailed definition of these parameters, refer to Ref. [17]. The theoretical fit result (which does not take the F–P interference effect into account) derived from this model is shown by the dashed line in Fig. 4. From Fig. 4 we can see that the overall feature of the theoretical model agrees with the experimental data, but there is a mismatch at the low energy level and high energy level, which indicates that there are other minor mechanisms contributing to emission besides Bremsstrahlung emission.

3.2. Light emission in the forward bias mode

This device can not only emit light under the reverse breakdown mode, but also under forward injection, with even lower voltage. Here we use the same structure as the above reverse-bias LED in the forward injection mode for low-voltage operation, which is favourable for the integration of Si-LED with CMOS IC power supplies. The DC current versus forward bias charactristic (I–V) and parasitic capacitance versus forward bias characteristic (C–V) are illustrated in Fig. 5.

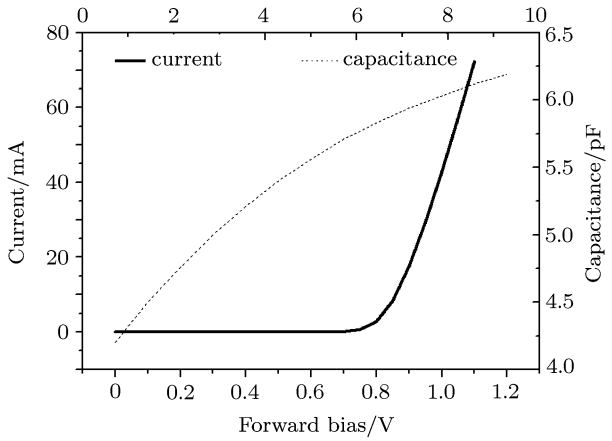


Fig. 5. The I–V and C–V characteristics of the device in forward bias mode.

As the operating voltage increases, the capacitance increases dramatically. The device in forward mode can emit light after turn-on voltage (about 0.7 V) and the spectrum of this device is spread over 800 nm to 1300 nm with seemingly split main peaks at 1116 nm (about 1.11 eV, near the band gap of silicon 1.12 eV) and 1150 nm (about 1.078 eV), and a minor peak at 1035 nm (about 1.2 eV), as shown in Fig. 6. The peak at 1116 nm takes a more dominant role and becomes sharpened as the current increases in comparison with the peak at 1150 nm, thus the possibility of the two split peaks due to the interference of surface passivation layer can be ruled out. The full width at half maximum (FWHM) is about 129 nm. The total optical power is about 12.5 nW at 1.2 V forward bias, 100 mA current, a little more than the optical power in the reverse bias mode at the same current. The electrical-to-optical conversion efficiency and EQE is about 1.04×10^{-7} and 1.12×10^{-7} respectively. Due to its low working voltage at same current and low absorption by bulk silicon at near infra-red (NIR) wavelength, it has lower power consumption and higher EQE (nearly one order higher) than that in reverse bias mode. However, as to internal quantum conversion efficiency, it is hard to estimate which one is better.

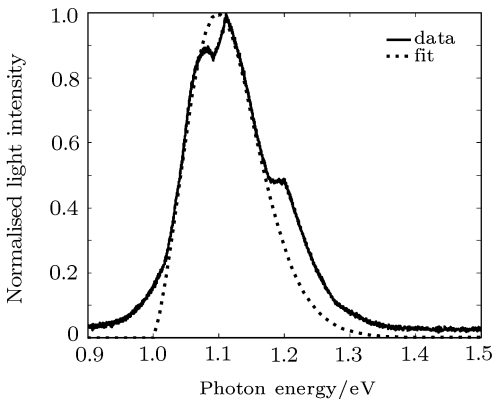


Fig. 6. EL spectra of the device in forward bias mode. Experimental spectrum: solid line; theoretical fit: dashed line.

In recent years many different experiments have obtained a similar main peak around 1130 nm[18,19] and different mechanisms were proposed to account for this phenomenon,[9,18–20] but with no definite conclusion. From the overall feature of the spectrume, the emission is a near band edge emission process. It is very similar to the line shape of the electron-hole-plasma (EHP) recombination model which has been reported to be the dominant mechanism in some indirect semiconductors (such as SiGe, AlGaAs, SiC, GaP). Thus EHP recombination is employed to fit the EL spectral line shape using the following expression:[21]

$$P(\hbar\omega) = I_0 \int_0^{\hbar\omega - E_g} \mathrm{d}E D_e(E) D_h(\hbar\omega - E_g - E) \times f(E, F_e, T) f(\hbar\omega - E_g - E, F_h, T), \quad (3)$$

where D_e and D_h are the densities of states of electron and hole, respectively, F_e and F_h are the respective quasi-Fermi energy, $\hbar\omega$ is the energy of the photon emitted, T is the measurement temperature, and $E_{g,EL}$ is the equivalent band gap energy of silicon by the EL measurement. From the physical viewpoint, this expression represents the convolution of the occupied electron and hole densities of state. The three-dimensional density of states $D(E) - E^{1/2}$ is used for holes, while a constant two-dimensional density of states is used for electrons in the accumulation layer. The quasi-Fermi energies for both electrons and holes in our simulation lie within the bandgap. Figure 6 shows the normalised theoretical EHP spectra, indicating an excellent fit to the normalised photoluminescence line shape.

The band gap $E_{g,EL}$ obtained from the EHP model is about 1.01 eV for the forward bias emission, lower than the Si band gap of 1.12 eV at room temperature. This can be accounted for as follows: in indirect gap semiconductors such as silicon, radiative interband transitions must be accompanied by the emission or the absorption of a phonon. This may lead to a large magnitude of radiative emission a phonon (or combinations of phonons) at energies less than the bandgap energy or slightly longer wavelength. Here only the conservation of energy is taken into account. The momentum conservation required by the indirect bandgap nature of Si is assumed to be provided by the scattering of the spread in the reciprocal space $-k$ space due to the localised wave function of electrons in the accumulation layer. Such a momentum spread effect may be caused by the traps between Si/SiO_2 interface,[9] impure nanoparticles or defects caused by ion implantation etc. Thus increasing the roughness of the interface between Si/SiO_2 is expected to have an enhancing effect on the light emission.[22]

Under all the above tests, poly-Si as the third terminal is floating. When the pn junctions of the device work under fixed bias conditions (eg. 1.2 V in forward bias) and certain bias (which is within the endurability of the gate) is applied to the poly-Si gate, the gate voltage has a modulation effect on the output light intensity of the device, and this modulation effect is more obvious in forward injection than that in reverse avalanche mode. Thus the gate modulation in the forward injection mode is our main focus. Figure 7 shows such a modulation effect under forward bias, from which we can see that below 1 V the modulation effect is barely detectable, and beyond 7 V, the gate oxide gate can be damaged permanently due to heat breakdown. Between 1 V–5 V, the integrated light intensity is almost linearly proportional to the applied gate voltage, and the output optical intensity is nearly doubled under a 5 V gate bias. During the modulation process, peaks of the emission and the shape of the spectra are basically unchanged. According to our estimation, the enhanced intensity is mainly ascribed to two reasons. One is that the applied positive gate voltage results in electron accumulation under the gate oxide accompanied by band bending. As a result the rate of minority carrier injection into the N-well is determined jointly by the p^+/N-well and gate/N-well biases. At a given pn forward bias, the injection rate could be significantly higher in a gated pn junction relative to a nongated junction. This phenomenon is very similar to the carrier barrier lowering effect that occurs in the lateral bipolar transistor.[23] The increased injection rate caused by the positive gate leads to increased emission power. The other reason is that the accumulation of electrons at the surface of the bulk silicon confines the photon emission to the surface of the device, thus absorption by silicon itself is reduced. As a result, the gated Si-LED has an obivous enhanced emission intensity.

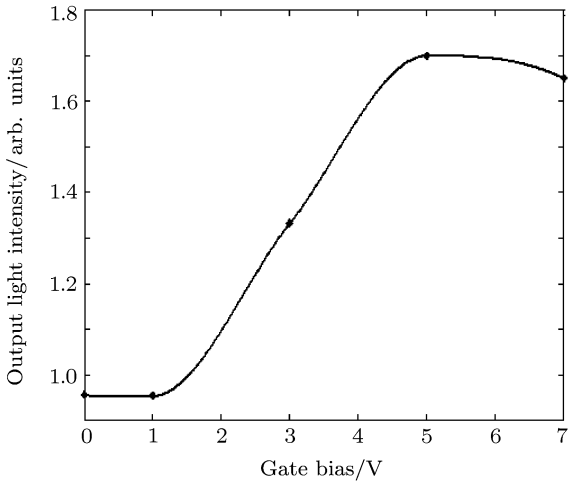


Fig. 7. Gate modulation effect on the output light intensity of the forward bias pn junction.

3.3. Light emission from the poly-Si/oxide/silicon structure

During the test of gate modulation effect, we also find that when the gate voltage is beyond about 7 V, the gate oixde is broken down suddenly under high electric field and there is current flowing through the gate and substrate even if a small voltage is applied to the poly-Si gate. The device gives off infrared light emission in this process. We measured the light emission in such a MOS structure or precisely poly-Si/oxide/silicon structure (all poly-Si connnected to positive voltage and all n^+ regions to the ground, as shown in Fig. 8). Its spectrum spreads from 900 nm to 1300 nm with peaks at 1116 nm (about 1.11 eV) and 1144 nm (about 1.084 eV), a minor peak at 1035 nm (about 1.2 eV), much similar to the emission peak in the above forward pn junction, except that the peak at 1144 nm (about 1.078 eV) seems to take a dominant role rather than 1116 nm (about 1.11 eV), as shown in Fig. 9. Light intensity in this mode is enhanced by 3–4 fold at the same current, in comparison with that in the aforementioned forward pn junction. This seems to indicate that the mechanism behind the

MOS structure is a little different from that in the forward pn junction. According to percolation theory,[24] there are many defect-induced traps dispersed in the oxide layer of a MOS structure. When a high electric field is applied to the poly-Si and substrate, the traps become overlapped. When these defects reach a critical density level, catastrophic breakdown occurs and there is conductance path between the poly-Si and the bulk silicon. The holes which go through the oxide into the valence band can relax to the band edge, and radiatively recombine with the electrons in the accumulation region if the momentum is conserved, as shown in Fig. 10. According to our assumption, there is surface band bending in the band diagram of the MOS structure under the accumulation condition, which can explain why the radiation peak energy in the MOS structure is lower than that in the pn junction. The possible physical mechanisms of MOS current in the high-current region may involve Schottky emission, Fowler–Nordheim tunneling, F–P emission etc.[25] Our MOS structure emission is very similar to that reported in Ref. [26]. But whether the mechanisms behind these two kinds of devices are same is still not resolved, since the oxide thickness of our device is estimated to be about 7 nm (ie. 1/50 of the minimum gate length[27]), a little thicker than the 2.4 nm thickness in Ref. [26]. For all assumptionss, there is no conclusive explanation and more work needs to be carried out to uncover the underlying mechanism.

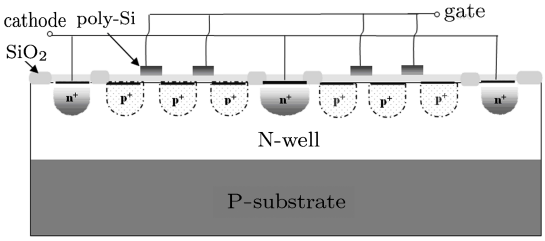


Fig. 8. The poly-Si/oxide/silicon structure.

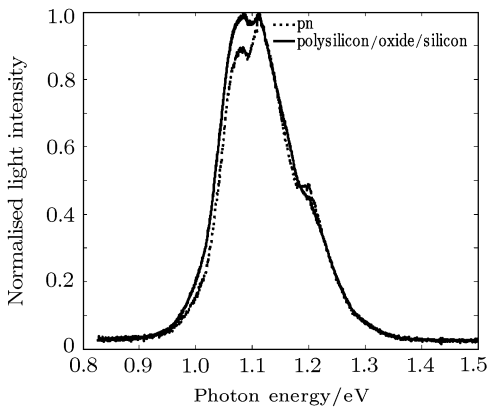


Fig. 9. EL spectra of the forward pn junction and poly-Si/oxide/silicon structure.

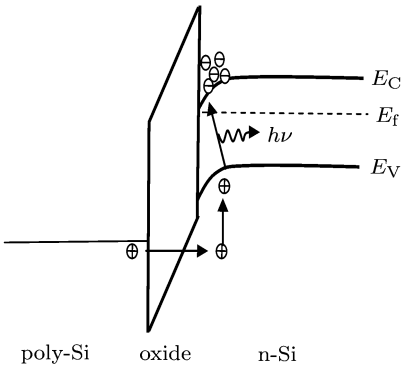


Fig. 10. The photon emission process for the poly-Si/oxide/silicon structure.

4. Conclusion

A novel three-terminal LED completely compatible with standard 0.35 μm CMOS technology is demonstrated in this paper. It is capable of multifunctional operations:

(i) It can emit light ranging from 500 nm to 1000 nm in reverse avalanche breakdown mode with a working voltage between 8.35 V–12 V;

(ii) It can emit infrared light ranging from 900 nm to 1300 nm in forward injection mode with a working voltage around 1 V; the poly-Si as the third terminal has an obvious modulation effect on the output optical intensity, especially in this mode;

(iii) When the voltage applied to the gate is in excess of its endurability, there is current flowing through SiO_2 between gate and substrate. Such a poly-Si/oxide/silicon structure can emit infrared light similar to that in a forward pn junction but with enhanced intensity.

All these possible working modes are realised in the same device structure. The pn junction based emission and MOS structure emission can be used either independently or cooperatively. The optoelectronic properties of this device working in different modes are characterised and compared. The characterisation of silicon-based pn junction LEDs not only has great significance in CMOS compatible light emission, but is also conducive to research on the various mechanisms behind silicon-based emission.[20,21,28] Thus this reasearch on multifunctional Si-LEDs in full CMOS technology can have profound significance in facilitating silicon's application in the optoelectronic domain. However this work only provides a prototype of Si-LEDs; there is much more scope for the optimisation of device performance and exploration of its potential applications.

References

[1] Cullis A G, Canham L T and Calcott P D J 1997 *J. Appl. Phys.* **82** 909

[2] Lu Z H, Lockwood D J and Baribeau J M 1995 *Nature* **378** 258

[3] Castagna M E, Coffa S, Monaco M, Caristia L, Messina A, Mangano R and Bongiorno C 2003 *Physica* E **16** 547

[4] Presting H, Kibbel H, Jaros M, Turton R M, Menczigar U, Abstreiter G and Grimmeiss H G 1992 **7** 1127

[5] Xu J, Ma T f, Li W, Chen K J, Li Z F and Lu W 2000 *Chin. Phys.* **9** 442

[6] Snyman L W, Aharoni H, du Plessis M and Gouws R B J 1998 *Opt. Eng.* **37** 2133

[7] Snyman L W, Aharoni H and du Plessis M 2005 *IEEE Phot. Technol. Lett.* **17** 2041

[8] Aaroni H and du Plessis M 2004 *IEEE Journal of Quantum Electronics* **40** 557

[9] Lee H C and Liu C K 2005 *Solid-State Electronics* **49** 1172

[10] du Plessis M, Aharoni H and Snyman L W 2002 *IEEE Journal of Selected Topics In Quantum Electronics* **8** 1412

[11] Newman R 1995 *Phys. Rev.* **100** 700

[12] Gautam D K, Khokle W S and Garg K B 1988 *Solid-State Electron* **31** 1119

[13] Figielski T and Torum A 1962 *International Conference on Physics of Semiconductors* Exeter UK, July 16–20 1962 p863

[14] Lacaita A, Zappa F, Bigliardi S and Manfredi M 1993 *IEEE Trans. Electron Dev.* **40** 577

[15] Akil N, Kerns S E, Kerns D V, Hoffmann A and Charles J P 1999 *IEEE Trans. Electron Dev.* **46** 1022

[16] Chynoweth A G and McKay K G 1956 *Phys. Rev.* **102** 369

[17] El Ghazi H, Jorio A and Zorkani I 2008 *Optics Communications* **281** 3320

[18] Ng W L, Lourenco M A, Gwilliam R M, Ledain S, Shao G and Homewood K P 2001 *Nature* **410** 192

[19] Green M A, Zhao J, Wang A, Reece P J and Gal M 2001 *Nature* **412** 805

[20] Lin C F, Liu C W, Chen M J, Lee M H and Lin I C 2000 *J. Appl. Phys.* **87** 8793

[21] Xiao X, Liu C W and Sturm J C 1992 *Appl. Phys. Lett.* **60** 1720

[22] Lee M H, Chen K F, Lai C C, Liu C W, Pai W W, Chen M J and Lin C F 2002 *Jpn. J. Appl. Phys.* **41** L326

[23] Joardar K 1994 *IEEE Trans. Electron Dev.* **41** 373

[24] Sez S M and Ng K K 2007 *Physics of Semiconductor Devices* (New Jersey: A John Willey & Sons, Inc.) p235

[25] Sez S M and Ng K K 2007 *Physics of Semiconductor Devices* (New Jersey: A John Willey & Sons, Inc.) p134

[26] Chang S T, Chen K F, Shie C R, Liu C W, Chen M J and Lin C F 2002 *Solid State Electronics* **46** 1113

[27] Sansen W M C 2006 *Analog Design Essentials* (Nertherlands: Springer) p9

[28] Le M P 2003 *Silicon Light Emitting Devices for Integrated Application* Ph. D. Thesis. University of Twente, Netherland